THE JOURNAL OF PHYSICAL CHEMISTRY B

Article

pubs.acs.org/JPCB

Role of Electrostatics in Differential Binding of RalGDS to Rap Mutations E30D and K31E Investigated by Vibrational Spectroscopy of Thiocyanate Probes

Christina M. Ragain, Robert W. Newberry, Andrew W. Ritchie, and Lauren J. Webb*

Department of Chemistry and Biochemistry, Center for Nano- and Molecular Science and Technology and Institute for Cell and Molecular Biology, The University of Texas at Austin, 1 University Station, A5300, Austin, Texas 78712, United States

Supporting Information

ABSTRACT: The human protein Rap1A (Rap) is a member of the Ras superfamily of GTPases that binds to the downstream effector Ral guanine nucleotide dissociation stimulator (RalGDS). Although Ras and Rap have nearly identical amino acid sequences and structures along the effector binding surface, the charge reversal mutation Rap K31E has previously been shown to increase the dissociation constant of Rap-RalGDS docking to values similar to that of Ras-RalGDS docking. This indicates that the difference in charge at position 31 could provide a mechanism for Ral to distinguish two structurally similar but functionally distinct GTPases, which would be of vital importance for appropriate biological function. In this report, vibrational Stark effect spectroscopy, dissociation constant measurements, and molecular dynamics simulations were used to investigate the role that electrostatic field differences caused by the charge reversal mutation Rap K31E play in determining the binding specificity of RalGDS to Rap versus Ras. To do this, six variants of RalGDS carrying a thiocyanate electrostatic probe were docked with three Rap mutants, E30D, K31E, and E30D/K31E. The change in absorption energy of the thiocyanate probe caused by RalGDS docking to these Rap variants was then compared to that observed with wild-type Ras. Three trends emerged: the expected reversion behavior, an additive behavior of the two single mutations, and cancelation of the effects of each single mutation in the double mutant. These observations are explained with a physical model of the position of the thiocyanate probe with respect to the mutated residue based on molecular dynamics simulations.

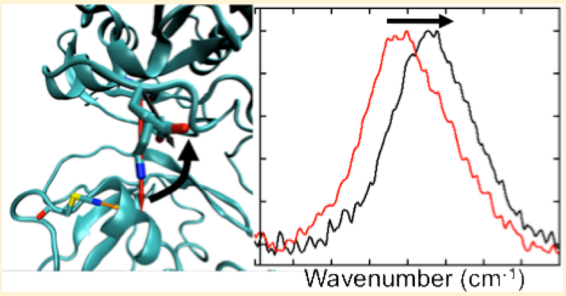

INTRODUCTION

The human proteins $p21^{Ras}$ (hereafter Ras) and Rap1A (hereafter Rap) are members of the Ras family of guanosine triphosphate (GTP)-hydrolyzing proteins that switch between an ON state when bound to GTP and an OFF state when bound to guanosine diphosphate (GDP) in the regulation of signal transduction pathways.[1] When in the GTP-bound ON state, both proteins dock to the Ras binding domain (RBD) of downstream effector proteins to propagate a signal transduction cascade. As members of the Ras superfamily of GTPases, Ras and Rap are similar in both sequence and structure; they share 50% amino acid identity[2] and 80% amino acid homology and have nearly identical structure and effector binding surfaces (root mean square (rms) deviation of 0.7 Å for homologous residues).

Despite these similarities, Ras and Rap have very different functions within the cell. Ras is involved in the propagation of chemical signals that regulate cell division, cell survival, and apoptosis and has been a focus of research in molecular oncology for many years.[3−5] The biological function of Rap is not as well understood, but it has recently been shown to play a role in cellular adhesion[6] and has been implicated in cancer metastasis.[7,8] The origin of the functional specificity of these two similar proteins lies in the ability of Ras and Rap to bind to different downstream effectors while in the GTP-bound ON state, thus initiating different signaling cascades. One of the best studied downstream effector proteins of Ras is the human protein c-Raf-1 (hereafter Raf), while Rap is thought to interact most strongly with the RBD of the downstream effector Ral guanosine dissociation stimulator (RalGDS, hereafter Ral). While the structures of the RBD of the downstream effector proteins are very similar,[2,9] measurements of free energies and equilibrium constants[10−13] of the protein−protein binding events indicate high specificity between the two GTPases and their appropriate downstream effector. Given the structural similarities of these protein−protein interfaces, a possible mechanism for the binding specificity that each GTPase shows for its appropriate downstream effector could be based on differences in electrostatic complementarity at the protein−protein interface. To investigate this hypothesis, the binding of these two GTPases to a variant of Ral has previously been investigated by our laboratory through both experimental and computational methods[12,14] in order to explore the contribu-

Received: April 5, 2012
Revised: June 15, 2012
Published: June 27, 2012

tion of electrostatic fields to interface formation in a system in which structural changes are limited as much as possible.

In 1995, Herrmann and co-workers[13,15] demonstrated the importance of the amino acids at positions 30 and 31 of Ras and Rap in discriminating downstream effector partners. These amino acids, Ras Asp 30 and Glu 31 and Rap Glu 30 and Lys 31, are positioned at the protein−protein binding interface, and studies involving reversion mutations of Rap to Ras have shown that these residues are involved in the interactions with downstream binding partners. Those studies found that the charge reversion mutation Rap K31E and the double mutation Rap E30D/K31E resulted in lowering the dissociation constant, K_d, between the Rap mutant and the downstream effector Raf to values similar to those of interactions between wild-type Ras and Raf.[15] Furthermore, the double mutant Rap E30D/K31E cocrystallized with the downstream effecter Raf, which usually binds more strongly to Ras. Similarly, the mutation Ras E31K was used to cocrystallize Ras with Ral, normally Rap's immediate downstream effector,[9] and the double reversion mutant Ras D30E/E31K has significantly reduced binding affinity with Raf.[16] The role of these mutations in creating strong binding affinity for an alternative downstream effector suggested an electrostatic mechanism caused by altering the charge of the residue at position 31 on either GTPase.

The arrangement of amino acid charges from secondary and tertiary protein structure can generate large and heterogeneous electrostatic fields that affect all protein function, including protein−protein interactions.[17−22] Vibrational Stark effect (VSE) spectroscopy is a recently developed experimental technique capable of measuring electrostatic fields in proteins.[23−30] In VSE spectroscopy, the intrinsic response of a probe vibrational oscillator to its local electrostatic environment is measured spectroscopically and is used to quantitate the magnitude and direction of the local electric field to which the probe is exposed. After calibration, the probe is inserted into a known position of a protein where it becomes a highly local, sensitive, and directional reporter of fluctuations of the protein's electrostatic field caused by structural or chemical perturbations to the protein. For example, the formation of a protein−protein interface through a docking interaction may induce changes in the absorption energy of a probe located on each protein surface as that probe is exchanged from an electrostatic field generated by the protein−water interface to one generated by the protein−protein interface.

The nitrile stretching vibration is one of several useful VSE probes that have been identified.[26] Several characteristics of the nitrile oscillator make it particularly attractive: its absorption energy of ∼2100−2250 cm^{-1} is in a region of the spectrum that is outside the vibrational background of a complex biomolecule, it is reasonably sensitive to fields of the magnitude thought to be present in proteins, and it can be incorporated into proteins with relative ease.[31] There are a growing number of reports describing VSE spectroscopy of nitrile probes to study the function of electrostatic fields in enzyme active sites.[25,27−30] Recently in our laboratory, VSE spectroscopy has been used to study the change in absorption energy of the nitrile probe incorporated at 11 locations on the surface of Ral that become buried in the protein−protein interface upon binding to either WT Ras or WT Rap.[12] This study determined that at some probe locations the change in absorption upon binding to WT Ras and WT Rap was similar, while at other locations the change was different, suggesting that these latter amino acids may participate in an electrostatic mechanism that enables Ral to distinguish Ras from Rap. Furthermore, measurement of the dissociation constant of the docking of the GTPases with nitrile containing Ral mutants showed no deleterious effect of the spectroscopic probe on the formation of the docked complex. These measurements were later confirmed through extensive molecular dynamics sampling of the protein−protein complex.[14] We hypothesized that several of these Ral-based nitrile probes would be ideal for investigating our hypothesis of an electrostatic mechanism for binding discrimination mediated by the charge on position 31 of these two GTPases.

In this report, we describe the systematic investigation of the effect of the E30D and K31E mutations to Rap on the local electrostatic fields in the downstream effector−GTPase complex measured by the nitrile probe at six locations on the surface of the RBD of Ral using VSE, molecular dynamics (MD) simulations, and dissociation constant (K_d) measurements. We selected six amino acids on Ral that are positioned in the protein−protein interface near positions 30 and 31 of Ras and Rap when the docked complex is formed: N27, G28, N29, Y31, K32, and N54. The locations of these amino acids within the Rap−Ral interface as well as Rap positions 30 and 31 are shown in Figure 1. Positions N27 and Y31 were selected

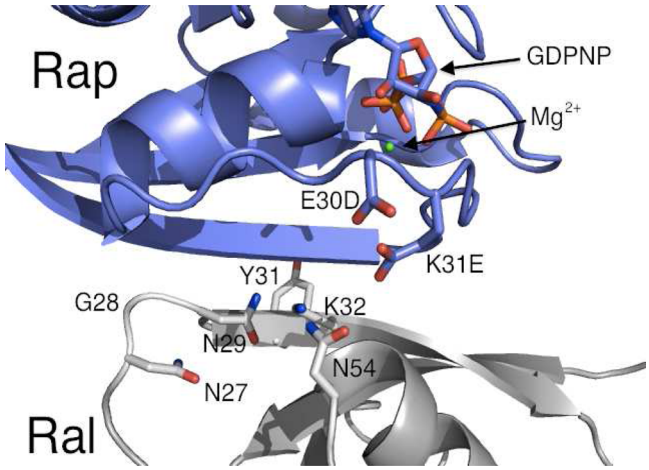

Figure 1. Rap (blue)−Ral (gray) interface highlighting Rap E30D and K31E and six amino acids on Ral that were selected for positioning the thiocyanate VSE probe in this study. The figure was prepared by aligning Rap from 1GUA[2] (containing the mutations E30D/K31E) to Ras docked with Ral from 1LFD.[43]

because at these probe locations, we previously measured a significant difference in the vibrational response of the thiocyanate between docking of the wild-type Ras and wild-type Rap[12] and wanted to investigate whether these observations were due to the different amino acid identity at positions 30 and 31. Position N29 was chosen because, along with position N27, molecular dynamics (MD) structural sampling of the thiocyanate side chain within the docked complex showed that the nitrile group has the largest angle with respect to the Ras−Ral interfacial plane of the collection of Ral-based probes we have investigated, approximately 45° from the plane of the Ras−Ral interface.[14] Because the observed effect of the change in electrostatic field is the projection of the field vector onto the nitrile probe bond axis, these positions seemed likely to respond to changes in the field vector at positions 30 and 31 of Rap, which appear from the crystal structures 1LFD[9] and 1GUA[2] to be approximately perpendicular to the interface. Gly28 was chosen as an intermediate between these two

dx.doi.org/10.1021/jp303272y | J. Phys. Chem. B 2012, 116, 9326−9336

residues. Finally, positions K32 and N54 were selected based on their physical proximity to the side chains of positions 30 and 31 on the GTPase once the docked complex formed.

Each of the six Ral amino acids was mutated to cysteine and then chemically modified to introduce the nitrile VSE probe in the form of the thiocyanate. These mutants were then bound to WT Rap, Rap E30D, Rap K31E, and the double mutant Rap E30D/K31E. The difference in vibrational absorption energy, $\Delta\nu_{obs}$, between the Ral monomer and the docked complex was measured by Fourier transform infrared spectroscopy (FTIR). The dissociation constant of the docked complex, K_d, was determined through a fluorescence assay. Finally, extensive MD simulations on docked complexes of all Rap and Ral variants were conducted to determine Boltzmann-weighted orientational data for the Ral-based nitrile probes and for the side chains at Rap positions 30 and 31. These simulations demonstrate that the mutation K31E is almost exclusively responsible for changes in side chain orientations at Rap positions 30 and 31 that cause the observed change in K_d. VSE spectroscopy demonstrates that only two of the probe locations examined, N27C and N29C, displayed a change in the absorption energy upon binding the Ras-like Rap double mutants that strongly resembled WT Ras. However, several of these probes did respond in an additive manner to the individual single mutations. These studies support both a structural and electrostatic mechanism to explain observed differences in GTPase−effector binding.

MATERIALS AND METHODS

A. Protein Expression and Purification. Gene constructs for WT Rap and WT Ral were synthesized and cloned into the pET-15b expression vector (Novagen) by GenScript (Piscataway, NJ) and the sequences confirmed. Amino acid mutations were made using the Quikchange mutagenesis kit (Stratagene) with PCR primers obtained from Sigma-Aldrich. The WT Rap construct was composed of residues 1−167 of Rap 1A. WT and mutant Rap vectors (Rap E30D, Rap K31E, and the double mutant Rap E30D/K31E) were transformed into *Escherichia coli* strain Arctic Express (DE) (Stratagene), and expression and purification were carried out as previously reported.[12] At the end of purification and loading with the nonhydrolyzable GTP analog guanosine 5′-[β,γ-imido]triphosphate trisodium salt hydrate (GDPNP, Sigma), Rap variants were exchanged into 50 mM tris (pH 7.5, 100 mM NaCl), hereafter termed "labeling buffer", for all further experiments. The WT Ral construct was composed of the 97-residue RBD of RalGDS, taken from residues 790−886. For clarity, we adopt the numbering convention of a RalGDS crystal structure, 1LFD, which indexes the glycine at position 797 in RalGDS as G14.[9] The mutations C16A and C17A were used to remove both wild type cysteines, generating a protein construct with no cysteine residues that we hereafter term Ralβ. Six amino acids were selected for mutation to cysteine, N27, G28, N29, Y31, K32, and N54. Expression and purification of Ralβ mutants followed previously established protocols.[12] All proteins were exchanged into the labeling buffer for all further experiments.

B. Introduction of the VSE Probe. The conversion of a cysteine thiol into the thiocyanate Stark probe has been described previously.[12,25] Three molar equivalents of 5,5′-dithiobis(2-nitrobenzoic acid) (DTNB, Sigma-Aldrich) were added to a Ralβ mutant containing one solvent-exposed cysteine residue and incubated at room temperature for 2−14 h, forming the protein-bound thionitrobenzoic acid disulfide. The extent of the reaction was monitored by observing the formation of the thionitrobenzoic acid (TNB) side product by its absorption at 412 nm. After 1 equiv of TNB had been generated, 30 equiv of potassium cyanide (KCN) was added to displace the protein-bound TNB and generate the protein−thiocyanate complex. The extent of the reaction was again observed by absorption of the TNB side product at 412 nm. At the end of the reaction, a PD-10 desalting column (GE Healthcare) was used to remove excess TNB and KCN and return the labeled protein to the labeling buffer. The SCN-labeled Ralβ mutants are denoted with the subscript, SCN.

C. Vibrational Stark Effect Spectroscopy. Infrared spectra of the six SCN-labeled Ralβ mutants bound to Rap E30D, Rap K31E, and Rap E30D/K31E were taken in the labeling buffer. To form the bound complex, the SCN-labeled Ralβ mutants were incubated with 1.2 molar equiv of one of the Rap mutants at 4 °C for 2 h. The solution was then concentrated by centrifugation to ∼2 mM. Vibrational absorption spectra of the bound complex were collected at room temperature in a sample cell composed of two sapphire windows separated by 125 μm thick PETE spacers in a Bruker Vertex 70 FTIR instrument. The sample cell was illuminated with light in the range of 2000−2500 cm^{-1} selected by a broad bandpass filter (Spectrogon, Parsippany, NJ) placed in front of the instrument's IR source. Spectra were composed of 250 scans collected with a liquid nitrogen-cooled indium antimonide (InSb) detector at 0.5 cm^{-1} resolution. The background-subtracted spectra were fit with a custom least squares fitting program to determine ν_{obs}; this is described in detail in the Supporting Information. Uncertainty in absorption energy is reported as the standard deviation of at least four measurements. Data for WT Ras and WT Rap were taken from an earlier published study.[12] The observed change in absorption energy of the thiocyanate, $\Delta\nu_{obs}$, was then compared to that of WT Rap and related to the change in the electrostatic environment in the vicinity of the probe caused by the protein−protein interaction, $\Delta\vec{F}_{dock}$, through eq 1

$$\Delta E = hc\Delta\nu_{obs} = -\Delta\vec{\mu}_{SCN}\cdot\Delta\vec{F}_{dock} \quad (1)$$

where $\Delta\vec{\mu}_{SCN}$, also called the Stark tuning rate, has been previously measured for the thiocyanate probe as 0.7 cm^{-1}/(MV/cm)[25] (i.e., a 1 MV/cm increase in electrostatic field upon docking will shift the absorption energy of the thiocyanate probe by −0.7 cm^{-1}). Uncertainty in $\Delta\nu_{obs}$ is reported as the linear propagation of uncertainty in ν_{obs}.

D. Dissociation Constant Measurements. Binding of the SCN-labeled Ralβ probes and Rap mutants was verified by observation of the docked complex by gel filtration and by measurement of the dissociation constant, K_d, of complex formation using a guanine nucleotide dissociation inhibition (GDI) assay described previously.[12,13] The GTPase (WT Ras, WT Rap, or Rap mutants) containing a fluorescently labeled GTP, 2′(or 3′)-O-(N-methylanthraniloyl)guanosine 5′-triphosphate trisodium salt (mant-GTP, Invitrogen), was incubated with varying concentrations of the RBD of interest (WT RalGDS or a SCN-labeled Ralβ mutant) at 4 °C for 1−2 h in a 96-well top reading fluorescence plate (Sigma). The dissociation of mant-GTP was initiated by the addition of 2.5 mM GDPNP. Decay in the fluorescence of mant-GTP was monitored in real time using a SpectraMax M3 multimode microplate reader (Molecular Devices) with excitation and emission wavelengths set to 365 and 450 nm, respectively. The

dx.doi.org/10.1021/jp303272y | J. Phys. Chem. B 2012, 116, 9326−9336

initial rate of this decay was taken to be the observed rate of the dissociation reaction and was fit as described previously to solve for K_d.[13]

E. Molecular Dynamics Simulations. Molecular dynamics simulations were carried out to determine probable orientations of each Ralβ-based thiocyanate probe and the side chains at Rap positions 30 and 31 with the Amber03 force field[32] using an umbrella sampling technique to generate a Boltzmann-weighted ensemble of structures. Amber03 simulation parameters for cyanocysteine and GDPNP were obtained from previous studies.[12,14] Starting from the Rap crystal structure 1GUA[2], a GSH tag left on the N-terminal methionine after cleavage of the hexahistidine affinity label during protein purification was modeled onto the N-terminus. This was done by searching the Protein Data Bank for proteins starting with the sequence GSHM (Met is the first Rap residue present in 1GUA). Obtained from pdbs, were 87 NMR structures and 1 crystal structure were obtained from the protein data bank (pdb): 1AQS (20 NMR structures),[33] 1W9R (19 NMR structures),[34] 2WCY (48 NMR structures),[35] and 2VKJ (1 crystal structure).[36] Rap was aligned to the methionine backbone of each GSHM structure using VMD,[37] creating 88 structures containing the GSHM N-terminus. After hydrogen atoms had been added using the GROMACS utility pdb2gmx,[38] an energy minimization was performed, and the lowest-energy structure from this collection was chosen as the Rap model to be used for further calculations. The SCN-labeled Ralβ mutants used for these simulations were obtained previously.[12] WT Rap was aligned by PyMol[39] to starting structures of the GTPase Ras E30K bound to the Ralβ mutants N27C_{SCN}, G28C_{SCN}, N29C_{SCN}, Y31C_{SCN}, K32C_{SCN}, and N54C_{SCN} created in a previous study.[14] Rap residues at positions 30 and 31 for each docked complex were mutated using AmberTools[32] to generate structures for Rap E30D, Rap K31E, and the double mutant Rap E30D/K31E, resulting in a total of 24 Rap−Ralβ structures. It was observed that in some structures, the N-terminal resides of Ralβ protruded between bonded atoms of Rap. To eliminate this nonphysical steric overlap, heavy atom restraints were placed on all amino acids but the Ralβ N-terminal GSHM residues and a 500-step gentle minimization was performed in Gromacs.[38] These were the initial structures for all molecular dynamics simulations.

From these starting structures, six additional structures were generated in which the cyanocysteine Cα-Cβ-Sγ-Cδ dihedral angle was fixed from 0° to 300° in 60° increments. These structures were then energy minimized, solvated by tip3p[40] in a dodecahedron box, and charge neutralized by the addition of sufficient Na^+ to eliminate the system charge. Finally, a 5000-step energy minimization was run on the entire system. All minimized structures containing each Rap variant docked to each SCN-containing Ralβ mutant were then subjected to 20 ps of MD simulation in order to relax the solvent. For each of these structures, molecular dynamics trajectories were initiated with the cyanocysteine Cα-Cβ-Sγ-Cδ dihedral angle (χ_2) restrained at each angle with a dihedral restraint potential that was flat within 30° of the center and quadratic with a force constant of 1000 kJ mol^{-1} rad^{-2} outside of that range. Six 3 ns trajectories with snapshots collected every 5 ps were generated for each mutant, for a total of 18 ns of simulation time per each Rap variant docked with each SCN-labeled Ralβ structure.

To test for structural rearrangements at positions 30 and 31 of Rap that would significantly influence the measured electrostatic field, the N−Cα-Cβ-Cγ dihedral angles (χ_1) on Rap residues 30 and 31 were each individually biased to create a Boltzmann-weighted ensemble of χ_1 rotomers. Rotomer libraries of WT Rap, Rap E30D, Rap K31E, and the double mutant Rap E30D/K31E were created using the strategy described above. Once again, structures containing dihedral angles from 0° to 300° in 60° increments were generated for each mutant; these were energy minimized, solvated in tip3p water, relaxed, and then sampled for 3 ns each, generating 18 ns of simulation for each biased torsional angle. To summarize, for 24 mutant-containing rotomer structures, MD sampling included 18 ns of simulation biasing the nitrile probe, 18 ns of simulation biasing of Rap position 30, and 18 ns of simulation biasing of Rap position 31, for a total of 1296 ns of MD simulation of this system.

The simulated torsional distributions were analyzed using the weighted-histogram analysis method (WHAM).[41,42] Each torsional angle was assigned to one of 72 5° bins ranging from −180° to 175°, and the probability (p_i) of finding a torsional angle in each bin (i) at 300 K was obtained as previously described.[14] In this way, a Boltzmann-weighted simulated distribution of structures was assembled in order to determine the average orientation of both the thiocyanate residues and the side chains at Rap positions 30 and 31 for comparison to experimental data. All simulations were analyzed for convergence by examining the WHAM-derived torsional distributions for the first half (0−9 ns) and the last half (9−18 ns) of the simulation. It was observed that, within reasonable variance due to the stochastic nature of MD, the simulated torsional distributions for each half were identical over the sampling time. These results are shown in Figure S1 of the Supporting Information.

Finally, control MD simulations of each Rap mutant docked with WT Ralβ (i.e., not containing the cyanocysteine mutation) were conducted in which the χ_1 dihedral angle for each unmutated residue at the probe location (Ral N27, N29, Y31, K32, and N54) was individually biased when docked with WT Rap and each Rap mutant. Because G28 does not have a χ_1 dihedral angle, an additional control simulation was sampled for 18 ns without bias while docked with each Rap construct. WHAM was again used to obtain a simulated Boltzmann-weighted distribution of the χ_1 dihedral angle for each WT Ralβ residue investigated here.

RESULTS

A. Dissociation Constant Measurements. Any effect of the thiocyanate probe on the formation of the interface can be investigated by comparing K_d values obtained for WT Ral versus the SCN-labeled Ralβ mutants docking to WT Ras and WT Rap; these are reported in Table 1. The dissociation constants presented in Table 1 demonstrate that the presence of the SCN probe on Ralβ mutants did not substantially affect binding to either WT Ras or WT Rap, as has been observed before.[12] The two largest deviations caused by Ralβ G28C_{SCN} (reduced K_d by an order of magnitude) and Ralβ Y31C_{SCN} (increased K_d by an order of magnitude) still showed an order of magnitude increase in K_d when binding to WT Ras as opposed to WT Rap, as is expected from our previous work. Along with results from molecular dynamics sampling of this system described below, this is strong circumstantial evidence that the nitrile VSE probe does not significantly alter the interface formed between Rap and the SCN-labeled Ralβ mutants compared to the WT interaction. Our experimental mutagenesis and chemical labeling strategy, therefore, does not

dx.doi.org/10.1021/jp303272y | J. Phys. Chem. B 2012, 116, 9326−9336

Table 1. Dissociation Constants, K_d, of the Formation of Docked Complexes of WT and SCN-Labeled Ralβ Mutants with GTPases under Investigation[a]

GTPase	WT	N27C$_{SCN}$	G28C$_{SCN}$	N29C$_{SCN}$	Y31C$_{SCN}$	K32C$_{SCN}$	N54C$_{SCN}$
WT Rap	0.26 ± 0.09	0.30 ± 0.05	0.04 ± 0.004	0.15 ± 0.08	1.0 ± 0.1	0.69 ± 0.18	0.91 ± 0.20
WT Ras	1.4 ± 0.2	7.3 ± 2.2	4.8 ± 1.1	3.1 ± 0.6	12.9 ± 4.8	6.0 ± 2.3	4.7 ± 0.4
Rap E30D	0.24 ± 0.06	0.12 ± 0.01	0.03 ± 0.015	0.10 ± 0.02	0.89 ± 0.35	0.34 ± 0.09	0.79 ± 0.10
Rap K31E	1.8 ± 0.7	2.9 ± 0.7	8.1 ± 1.5	6.0 ± 1.1	6.2 ± 2.0	1.9 ± 0.8	2.2 ± 1.5
Rap E30D/K31E	1.0 ± 0.1	5.4 ± 1.0	2.5 ± 0.3	5.0 ± 1.7	2.0 ± 0.2	1.8 ± 0.5	1.1 ± 0.3

[a]All values are reported in micromolar, and errors represent one standard deviation from multiple experiments.

destroy the protein−protein interaction that we are attempting to measure.

Table 1 also shows that binding of WT Ral to WT Rap was approximately 10-fold faster than binding to WT Ras, as has been reported before.[12,13,15] These results confirm previous reports that the reversion mutation at Rap position 31 alters the binding interaction between Rap and Ral to resemble that of Ras and Ral. All SCN-labeled Ralβ mutants interacted with Rap K31E with a K_d 10-fold higher than with WT Rap, and this effect was preserved in the double mutant Rap E30D/K31E. The single mutation Rap E30D had no effect on binding, and all K_d values measured with that construct were essentially identical to that of WT Rap. It is therefore clear that the amino acid located at position 31 of the GTPase is critical in the mechanism that enables Ral to distinguish structurally similar but functionally distinct GTPases for appropriate binding. Exploring the structural and electrostatic components of that mechanism is the subject of the MD sampling and VSE spectroscopy discussed here.

B. Molecular Dynamics Simulations. The structure of the interface formed between Rap and Ral has been investigated with two high-quality crystal structures, 1GUA and 1LFD.[2,9] These are crucial starting points for any comprehensive biochemical understanding of the Rap−Ral interactions, but the static structures of these proteins might not represent the full range of side chain conformations of either our SCN probe or positions 30 and 31 of the GTPase and so are not sufficient for our purposes. Furthermore, our experiments were conducted with an unnatural variant of the system, the SCN-labeled Ralβ mutant. Although our K_d measurements indicate that the presence of the thiocyanate probe does not significantly disrupt interface formation, knowledge of the orientation of the probe within the interface is necessary to interpret vibrational absorption data since the change in nitrile frequency is caused by the projection of an electrostatic field onto the difference dipole moment of the nitrile, which is parallel to the carbon−nitrogen triple bond. A single random or handpicked assignment for the thiocyanate orientation therefore potentially introduces a large systematic error in the interpretation of the experimental data. To address these issues, we performed extensive molecular dynamics sampling of each SCN-labeled Ralβ mutant docked with WT Rap and the Rap mutants E30D, K31E, and E30D/K31E to accumulate a Boltzmann-weighted ensemble of simulated orientations of the thiocyanate group and the side chains at Rap positions 30 and 31. By examining an ensemble of structures obtained from stochastic dynamic sampling, we have accumulated a range of possible structures that could be induced by atomic-level changes in all experimental mutants while limiting errors in probable structures due to choices made about the system, such as starting structure orientations. The end result is a set of snapshots that represent an ensemble of structures that could be present during our room temperature steady-state experiment, rather than a small number of crystal structures that are not likely to exist in significant populations.

The WHAM-derived χ_2 simulated torsional probability distribution for all thiocyanate groups and χ_1 torsional probability distribution side chains at Rap positions 30 and 31 are shown in Figures S2−S4 of the Supporting Information. Similar to what we have seen previously,[14] the torsional distributions for all of these side chains were characteristic of an unhindered alkyl group, with three probability maxima separated by ∼120° and essentially no significant difference depending on the chemical identity of either the SCN-labeled Ralβ mutant (Figure S2 of the Supporting Information) or the Rap variant (Figures S3 and S4 of the Supporting Information) in the docked complex. Our MD sampling strategy therefore provides us with a comprehensive ensemble of structures of each docked Rap−Ralβ variant studied with VSE spectroscopy to aid in interpreting our spectroscopic results.

To analyze our molecular dynamics simulations of the torsional distribution of the thiocyanate residue on each Ralβ mutant and of the amino acids at Rap positions 30 and 31, we defined two angles for each side chain with respect to the Rap−Ralβ surface, which we term azimuthal (θ) and polar (ϕ) angles. These two angles, as well as our method of obtaining Boltzmann-weighted averages of both angles, are described in the Supporting Information and are shown schematically in Figure 2. Figure 2A defines a surface plane at the interface of Rap (above the plane) and Ral (below the plane); azimuthal angles are reported relative to this plane. When the crosshairs in Figure 2B are translated to the Cα atom of each simulated residue on Rap (represented as spheres) or Cδ atom on Ralβ, they become the origin of the polar angles shown in Figures 3 and S5 of the Supporting Information. The average azimuthal and polar angles of the nitrile probe relative to the Rap−Ralβ binding interface are shown in Figure S5 of the Supporting Information. These simulations were compared with previous simulations of the Ras−Ralβ binding interface,[14] and in all cases, the orientations of the nitrile at the docked interface for Ras and Rap are identical, within the error distribution of the simulated Boltzmann-weighted ensemble. This indicates that the structure of the probe at the interface of these two GTPases is very similar, as expected by the structural similarities of the crystal structures, the amino acid homology of the GTPases, and the fact that the measured K_d values of the SCN-labeled Ralβ mutants dock with Ras and Rap with the same dissociation constant as WT Ral. Furthermore, as seen in Figure S5 of the Supporting Information, mutations to positions 30 and 31 of Rap did not substantially alter the orientation of the nitrile probe at the interface. The consistency of the probe orientation in these Boltzmann-weighted ensembles is further evidence that this protein−protein interface is suitable for systematic

dx.doi.org/10.1021/jp303272y | J. Phys. Chem. B 2012, 116, 9326−9336

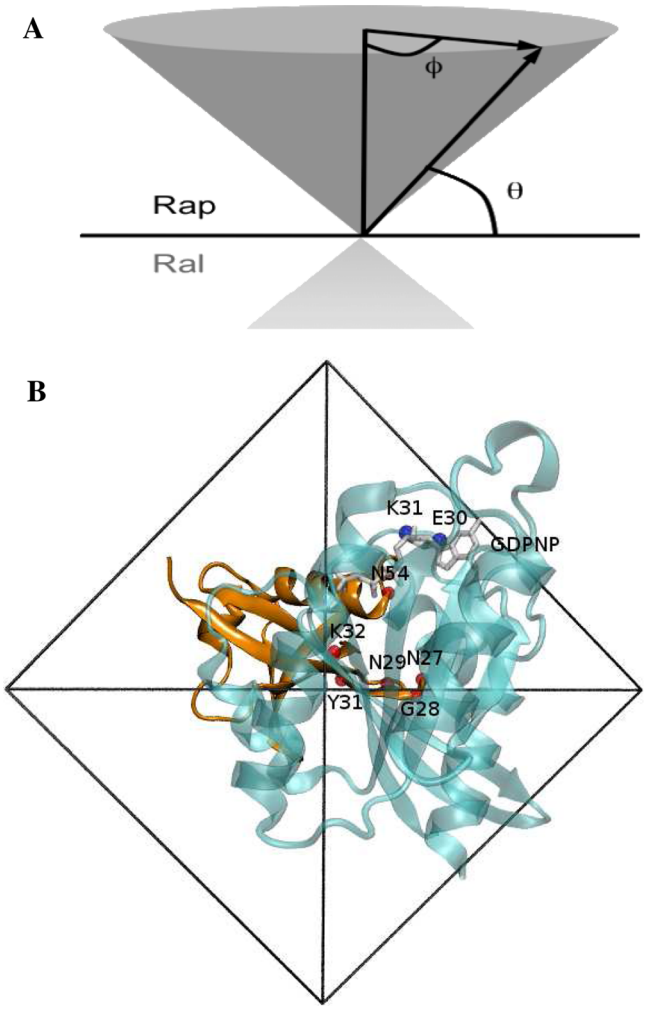

Figure 2. Representation of the azimuthal (θ) and polar (ϕ) angles for the residues discussed here. (A) The surface plane was defined by the average of the plane fit with all Cα atoms. Azimuthal angles are shown relative to this plane, where Rap is above the plane and Ral is below the plane. (B) Representation of the polar angle. Translating the black crosshairs to the Cα of each residue (represented by spheres) determines the origin of the polar angles presented in Figure 3 and S4 of the Supporting Information. Rap is shown in blue and Ral in orange.

measurements with the nitrile vibrational probe without compromising the structural integrity of the interface.

The azimuthal and polar angles of the side chains at Rap positions 30 and 31 for each mutant studied here are shown in Figure 3. Upon examination of position 30 (Figure 3A), the azimuthal angles showed essentially no difference depending on either the Rap mutant or the SCN-labeled Ralβ mutant to which it was docked. In all cases, the aspartate (for E30D and E30D/K31E) or glutamate vector (for WT and Rap K31E) pointed approximately parallel and slightly below the Rap−Ral surface plane. Similarly, the polar angles of the side chain at position 30 (Figure 3B) showed only minor random fluctuations that resulted from WHAM-derived standard deviations. This suggests that both aspartate and glutamate side chains at this position undergo limited polar motions that are not influenced by the chemical identity of position 31 or the location of the thiocyanate probe.

The side chains at Rap position 31 behaved very differently. The azimuthal angles of the side chain at Rap position 31 (Figure 3C) were pointed significantly further below the Rap−Ralβ mutant plane than at position 30 (55−60° below the surface plane for position 31 versus approximately parallel to the surface plane for position 30). Unlike azimuthal angles seen at position 30, for which all Rap mutants behaved identically, WT Rap and Rap E30D behaved identically, while the Rap mutants K31E and E30D/K31E behaved identically. This is most apparent when these Rap constructs were docked with N29C$_{SCN}$, Y31C$_{SCN}$, and N54C$_{SCN}$, but the trend is apparent for all docked complexes. Furthermore, the simulated distribution of polar angles of mutants of Rap position 31 displayed a significant dependence on the identity of the residue at position 31 (Figure 3D). Again, WT Rap and the Rap E30D behaved identically, while the Rap mutants K31E and E30D/K31E behaved identically. Taken together, the data presented in Figure 3 strongly support the evidence that mutations at Rap K31 are most important for causing structural changes that might effect Rap binding to the downstream effector Ral, and mutations to Rap E30 do not significantly affect the structure of either WT Rap or Rap K31E. Both of these observations are consistent with differences in K_d between WT and mutated Rap binding to the downstream effector Ral.

We investigated the causes of the difference in orientation between the lysine and glutamate side chains at Rap position 31 through inspection of representative MD snapshots collected from sampling trajectories. This clearly revealed that when a lysine was at position 31, it pointed toward a hydrogen bonding acceptor pocket formed by Ralβ D51, N54, and E58. When this side chain was mutated to Rap K31E in either the single or double mutant, the negatively charged Glu reoriented to avoid electrostatic repulsion with this hydrogen bond accepting pocket. This appears to be the central cause for both the dissociation constant and electrostatic differences between Rap−Ralβ binding and Ras−Ralβ binding described here. Although N54C$_{SCN}$ broadly followed this pattern as seen in Figure 3D, the polar angles of the residue at position 31 in K31E and E30D/K31E varied more significantly than with the other mutants. Inspection of MD structures showed that when the nitrile probe was located at N54C$_{SCN}$, the nitrile disrupted the hydrogen bonding pocket sufficiently to cause this portion of the Ralβ surface to retract slightly from the Rap−Ralβ interface, leaving K31 without these hydrogen bonds. Although the importance of this hydrogen bonding pocket can be hypothesized from the 1LFD crystal structure, our MD sampling has provided the first confirmation of the observed biochemical behavior of Ras and Rap with direct structural evidence.

Finally, we performed control simulations on the unmutated Ralβ docked with WT Rap and each Rap mutant in order to determine the effect that the cyanocysteine mutation might have on the overall structure of the docked complex. We compared two general measurements of the structure around each mutated residue to the control simulations: (1) the number of hydrogen bonds that surround the site and (2) the backbone rms deviation for residues within 20 Å of the site's Cα. No significant difference between docked complexes containing Ralβ or SCN-labeled Ralβ mutants was found. These control simulations are described extensively in the Supporting Information, and results are shown in Figures S6 and S7 of the Supporting Information.

C. VSE Spectroscopy of the Docked Protein−Protein Complex. *Ralβ N27C$_{SCN}$ and N29C$_{SCN}$.* The selection of six SCN-labeled Ralβ probes was based on consideration of each probes' orientation compared to the Rap−Ralβ interface,

dx.doi.org/10.1021/jp303272y | J. Phys. Chem. B 2012, 116, 9326−9336

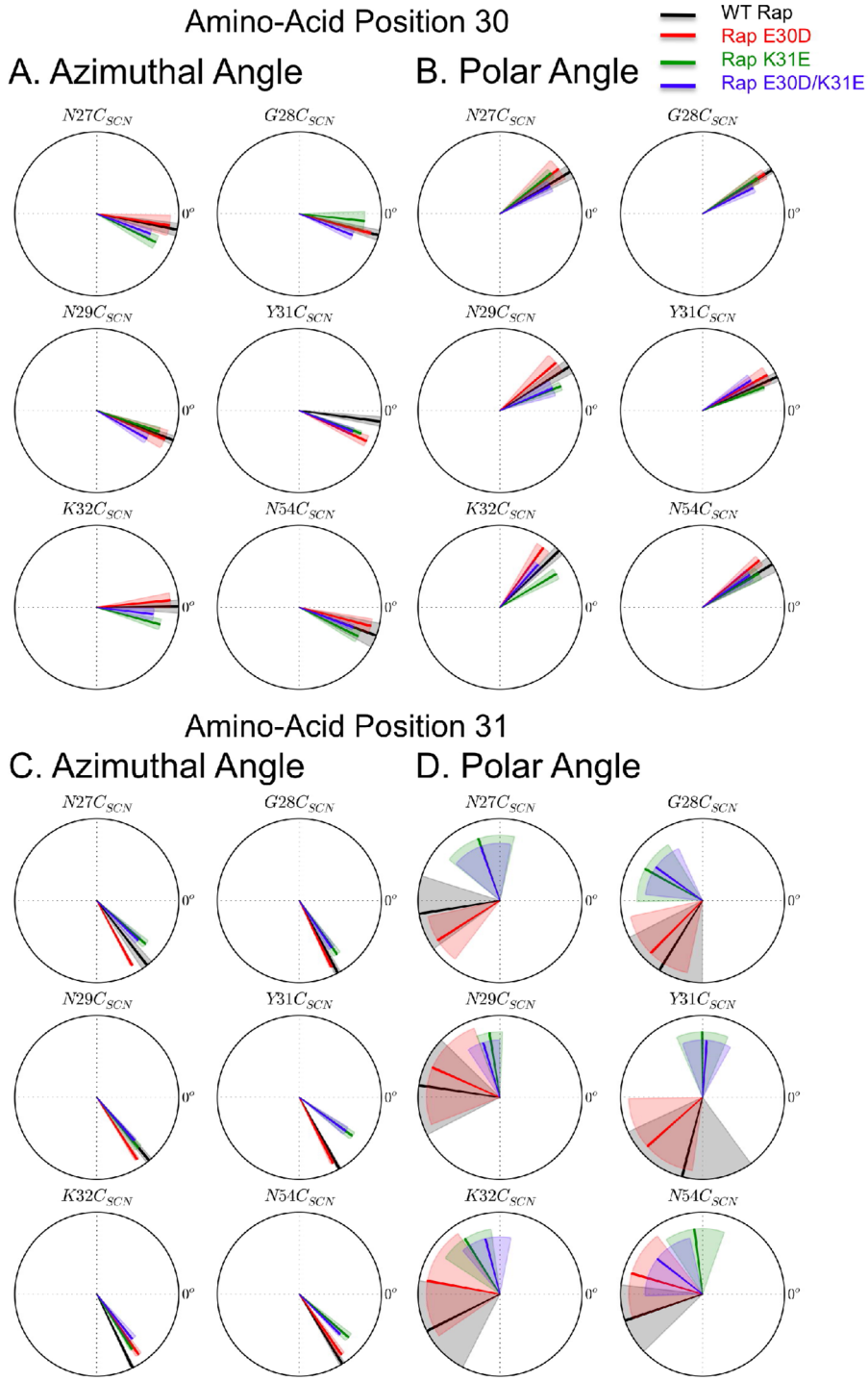

Figure 3. Azimuthal and polar angles of the side chain at Rap positions 30 and 31 in WT Rap (black), Rap E30D (red), Rap K31E (green), and Rap E30D/K31E (blue). (A) Azimuthal angle at Rap position 30. (B) Polar angle at Rap position 30. (C) Azimuthal angle at Rap position 31. (D) Polar angle at Rap position 31. Azimuthal angles are shown relative the Rap−Ral surface plane. Polar angles are shown relative to the coordinate system shown in Figure 2B. The shaded area represents the variance of the calculated angle from the Boltzmann-weighted ensemble of structures, described in the Supporting Information.

proximity to Rap positions 30 and 31, and large differences in vibrational absorption energy upon binding to WT Ras and WT Rap measured in a previous study.[12] $N27C_{SCN}$ and $N29C_{SCN}$ were selected for probe locations because our Boltzmann-weighted molecular dynamics simulations of the orientations of the six thiocyanate probes when docked with each of the Rap constructs determined that the thiocyanate group on these two Ralβ mutants had some of the largest angles with respect to the plane of the WT Rap−Ralβ interface of any of our probes, approximately 20−30° above the surface plane (Figure S5A of the Supporting Information).[14] Because VSE spectroscopy is only sensitive to changes in the electrostatic field vector projected onto the nitrile bond axis and mutations to Rap K31 were themselves close to perpendicular to the Rap−Ralβ surface plane as shown in Figure 3C, probes perpendicular to

dx.doi.org/10.1021/jp303272y | J. Phys. Chem. B 2012, 116, 9326−9336

the Rap−Ralβ plane would be most sensitive to mutations to Rap K31.

An example of the VSE data collected here is shown in Figure 4. The Ralβ N29C$_{SCN}$ mutant was incubated with each

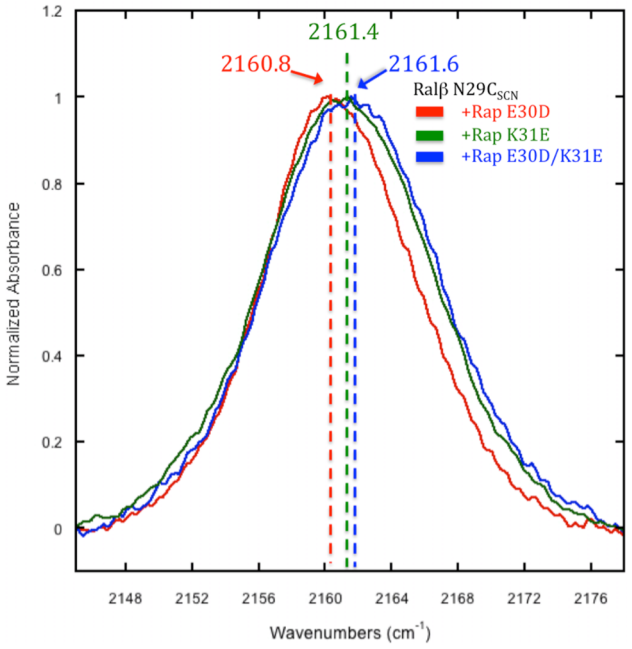

Figure 4. Normalized absorbance of thiocyanate on Ralβ N29C$_{SCN}$ measured when docked with Rap E30D (red, 2160.8 cm^{-1}), Rap K31E (green, 2161.4 cm^{-1}), and Rap E30D/K31E (blue, 2161.6 cm^{-1}).

Rap mutant, concentrated, and the absorption energy of the nitrile probe was recorded and compared with the measured absorption energy when bound to WT Rap from a previous study.[12] When the thiocyanate was docked with Rap E30D, its absorption energy was 2160.8 cm^{-1}, identical to the observed absorption energy when Ralβ N29C$_{SCN}$ was bound to WT Rap. When Ralβ N29C$_{SCN}$ was incubated with Rap K31E, the absorption energy increased by 0.6 cm^{-1}, to 2161.4 cm^{-1}. However, when thiocyanate was docked with the double mutant, Rap E30D/K31E, its absorption energy shifted 0.8 cm^{-1} higher in energy (2161.6 cm^{-1}). The absorption energies of both Rap mutants containing K31E were therefore more similar to the observed absorption energy when Ralβ N29C$_{SCN}$ was docked with WT Ras (2161.1 cm^{-1}) than with WT Rap. This indicates that the probe is experiencing an electrostatic environment in the double mutant E30D/K31E that is more like that of WT Ras than WT Rap.

Changes in the absorption energy ($\Delta\nu_{obs}$) of the thiocyanate on each SCN-labeled Ralβ mutant due to binding to Rap constructs are summarized in Table 2 and Figure 5. Data for the fitted center and fitted full width at half-maximum (fwhm)

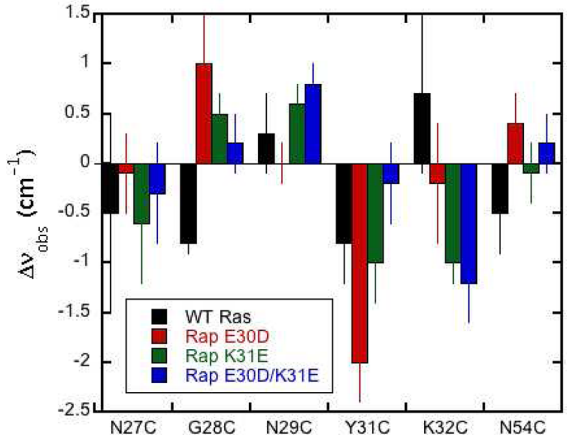

Figure 5. Change in absorption energy compared to WT Rap, $\Delta\nu_{obs}$, of a nitrile probe on SCN-labeled Ralβ mutants when bound to WT Ras (black), Rap E30D (red), Rap K31E (green), and Rap E30D/K31E (blue) where $\Delta\nu_{obs}$ = 0 represents no change from the thiocyanate absorption energy when bound to WT Rap reported in Table 2. Error bars represent the propagation of error of ν_{obs}.

of each peak are given in Table S1 of the Supporting Information. In these figures and tables, $\Delta\nu_{obs}$ values are referenced to the absorption energy of the nitrile probe when docked with WT Rap (i.e., $\Delta\nu_{obs}$ = 0 represents no change from the thiocyanate absorption energy when docked with WT Rap).[12]

When the probe is located at Ralβ N27C$_{SCN}$ and N29C$_{SCN}$, the data in Figure 5 clearly show that both the single and double reversion mutants Rap K31E and E30D/K31E have nitrile absorption energies that are similar to that of WT Ras, not WT Rap. In both cases, the single mutation Rap E30D appears to have a negligible effect on the electrostatic environment of the probe. At these particular probe locations, therefore, the double mutation does indeed revert the electrostatic field of Rap back to that found in Ras. Although these energy shifts are small, the trend toward higher absorption energies, when bound to WT Ras and the double mutant Rap E30D/K31E than when bound to WT Rap, is clear. The relatively small effect of mutations on the magnitude of the absorption energy of Ralβ N29C$_{SCN}$, in particular, may be due to the fact that the azimuthal angles of the Rap mutants all decreased relative to that of WT (Figure S5 of the Supporting Information), possibly eliminating the utility of this probe position.

Table 2. Measured Vibrational Frequencies of SCN-Labeled Ralβ Mutants Docked with WT Rap[a]

GTPase		N27C	G28C	N29C	Y31C	K32C	N54C
WT Rap	ν_{obs} (cm^{-1})	2162.6 (0.4)	2161.8 (0.1)	2160.8 (0.2)	2161.5 (0.2)	2160.9 (0.2)	2161.4 (0.2)
		Difference Compared to WT Rap					
WT Ras	$\Delta\nu_{obs}$ (cm^{-1})	−0.5 (1.0)	−0.8 (0.1)	0.3 (0.4)	−0.8 (0.4)	0.7 (0.8)	−0.5 (0.4)
Rap E30D	$\Delta\nu_{obs}$ (cm^{-1})	−0.1 (0.4)	1.0 (0.5)	0.0 (0.2)	−2.0 (0.4)	−0.2 (0.6)	0.4 (0.3)
Rap K31E	$\Delta\nu_{obs}$ (cm^{-1})	−0.6 (0.6)	0.5 (0.2)	0.6 (0.2)	−1.0 (0.4)	−1.0 (0.2)	−0.1 (0.3)
Rap E30D/K31E	$\Delta\nu_{obs}$ (cm^{-1})	−0.3 (0.5)	0.2 (0.3)	0.8 (0.2)	−0.2 (0.4)	−1.2 (0.4)	0.2 (0.3)

[a]The observed changes in vibrational frequency ($\Delta\nu_{obs}$) upon docking each probe to WT Ras, Rap E30D, Rap K31E, and Rap E30D/K31E. Error in ν_{obs} is reported as one standard deviation from multiple experiments and error in $\Delta\nu_{obs}$ is reported as the propagation of error in ν_{obs}.

dx.doi.org/10.1021/jp303272y | J. Phys. Chem. B 2012, 116, 9326−9336

K32C$_{SCN}$ and N54C$_{SCN}$. Figure S5A of the Supporting Information shows that the azimuthal angle of nitrile probes at positions K32C$_{SCN}$ and N54C$_{SCN}$ also positioned them above and approaching perpendicular to the interfacial plane. These two residues are also near Rap positions 30 and 31 when the docked complex forms. The closest Ralβ amino acid to positions 30 and 31 is N54 (a distance from backbone atoms of approximately 11−16 Å in our Boltzmann-weighted ensemble of structures). As shown in Figure 5, the two single mutations E30D and K31E have small but opposite effects on the absorption energy of N54C$_{SCN}$ when compared to WT Rap; Rap E30D is 0.4 cm^{-1} higher in absorption energy while Rap K31E is 0.1 cm^{-1} lower in absorption energy. The combined effect of the double mutant Rap E30D/K31E, however, gave a VSE shift 0.2 cm^{-1} higher in energy than WT Rap, resulting in an absorption energy that was approximately the sum of the shifts caused by the two single mutations. As discussed above, because N54C$_{SCN}$ visibly disrupted the hydrogen bonding interaction with Rap K31 in the docked complex, it is likely that the structural disruption of this interface means that this position is not appropriate for deconvoluting structural and electrostatic effects. This observation demonstrates the importance of investigating both structural and electrostatic contributions to the biochemical question of interest.

The nitrile vibrational probe was placed at Ralβ K32C$_{SCN}$ because of its proximity to positions 30 and 31 on the GTPase in the docked complex. As can be seen in Table 2 and Figure 5, although the measured error in $\Delta\nu_{obs}$ was larger than at other positions, there was a dramatic effect of the mutation Rap K31E on the absorption energy of the thiocyanate compared to WT Rap (−1.0 cm^{-1}), while Rap E30D caused only a small perturbation (−0.2 cm^{-1}). The behavior of the double mutant Rap E30D/K31E was the sum of these two shifts, −1.2 cm^{-1}. This was very different from the response on binding to WT Ras, which showed a shift in absorption energy of +0.7 cm^{-1} compared to WT Rap. These two probe locations responded to the double mutant Rap E30D/K31E essentially as the addition of electrostatic changes caused by each single E30D and K31E mutation. However, in neither case did the double reversion mutation to Rap produce an electrostatic environment measured by the probe that was similar to Ras.

G28C$_{SCN}$ and Y31C$_{SCN}$. We chose Ralβ G28C$_{SCN}$ as a probe location because it was between positions N27 and N29, even though it did not meet other desirable criteria. Previous studies had shown that probes at this location have very little sensitivity to differences in binding to WT Ras versus WT Rap[12] and a position in the docked complex that was more consistently parallel to the surface than either N27C$_{SCN}$ or N29C$_{SCN}$.[14] Even still, this probe did respond strongly to mutants Rap E30D and K31E (+1.0 and +0.5 cm^{-1} versus WT Rap, respectively), compared to a shift of −0.8 cm^{-1} when bound to WT Ras. The double mutant, Rap E30D/K31E, however, only demonstrated a shift of +0.2 cm^{-1} compared to WT Rap. The probe at this location thus reacted in a manner in which the two single mutations appear to cancel each other out. After extensive inspection of our MD simulations, we have found no significant structural differences near G28C$_{SCN}$ to explain this observation. It could be that the distance between G28 and the region of the binding surface we are investigating by mutations at Rap E30 and K31 makes Ralβ G28C$_{SCN}$ an ineffective probe for this study. This result is noteworthy, however, because the distance over which linear VSE effects can be accurately measured has still not been experimentally established.

Position Ralβ Y31C$_{SCN}$ was selected for study because the change in absorption energy upon docking to WT Rap differed from WT Ras by a large amount, 0.8 cm^{-1}. As shown in Table 2, both single mutants Rap E30D and Rap K31E shifted the absorption energy of the nitrile probe on Ralβ Y31C$_{SCN}$ to lower energy, by −2.0 and −1.0 cm^{-1}, respectively. However, the combined effect of the double mutant was to shift the absorption energy lower by only −0.2 cm^{-1} compared to WT Rap, substantially less than either single mutant. As shown in our molecular dynamics simulations (Figure 3D), there is a significant reorientation of the side chain at position Rap 31 above (azimuthal angle) and away from (polar angle) Ralβ Y31C$_{SCN}$ in the mutants Rap K31E and E30D/K31E, which is likely causing this probe to become significantly less sensitive to the kinds of changes in the electrostatic field of the binding region in which we are interested.

DISCUSSION

This study was motivated by functional observations that positions 30 and 31 of Ras and Rap, which are among the few chemical differences between the Ras and Rap interfaces, could help discriminate appropriate downstream effectors for each GTPase. Because of the structural similarities of these two protein surfaces, it is possible that downstream effector binding selectivity could be caused by changes in the electrostatic fields at the GTPase−effector interface caused by mutations at positions 30 and 31 and, in particular, by the reversal of charge caused by the K31E mutation. Measuring this effect from the perspective of the downstream effector Ral, which can bind to both GTPases, proved useful for exploring this aspect of GTPase function. Previous experimental work and extensive MD sampling provided us with criteria to guide the selection of positions for the nitrile probe on the Ralβ surface. These criteria were (1) the angle of the nitrile with respect to the GTPase−effector interface, with probes perpendicular to the plane of the interface preferred (N27C$_{SCN}$ and N29C$_{SCN}$), (2) proximity to positions 30 and 31 when the docked complex is formed (K32C$_{SCN}$ and N54C$_{SCN}$), and (3) previously measured discrimination in absorption energy when docking to Ras as opposed to Rap, indicating that those probes end up in significantly different electrostatic environments after the docked complex is formed (N27C$_{SCN}$, N29C$_{SCN}$, and Y31C$_{SCN}$). The location G28C$_{SCN}$ was chosen because of its position between N27C$_{SCN}$ and N29C$_{SCN}$, not because of any useful selection criteria, and could be considered as a control location on the Ralβ surface. No probe was an ideal experimental tool in all three selection criteria, and some probes were ideal in one experimental consideration but problematic in another. For example, the azimuthal angles of N27C$_{SCN}$ and N29C$_{SCN}$ were ideal, but the distances of these two probes from Rap positions 30 and 31 in the docked complex were large. Even with detailed structural and electrostatic information, the limitations of the biological system do not allow us to design a perfect experiment; all probes will experience a convolution of ideal and problematic characteristics, and all probes will be unique. Therefore, electrostatic fields must be explored from the perspectives of multiple probes and information taken from the aggregation of the data.

We observed three general trends from the six probe locations studied. The first was seen with N27C$_{SCN}$ and

dx.doi.org/10.1021/jp303272y | J. Phys. Chem. B 2012, 116, 9326−9336

$N29C_{SCN}$, which displayed the Rap-to-Ras reversion behavior caused by the double mutation Rap E30D/K31E. The absorption energy of this double mutant essentially matched that of WT Ras and in both cases was caused almost exclusively by the mutation K31E, not E30D. This is direct confirmation of hypotheses proposed from previous crystallographic and docking studies that the difference between Ras and Rap at these two positions leads to the functional discrimination these two GTPases have for different downstream effectors. The second observed trend was that of the double mutant displaying a difference in absorption energy that was simply the sum of the effect caused by the two single mutations. This was seen at positions $K32C_{SCN}$ and $N54C_{SCN}$. This is strong experimental evidence that these mutations cause very little disruption in the docked complex and experience additive changes in the electrostatic field that can be measured by VSE spectroscopy of appropriately placed probes. However, it is important to study these effects from as many different probe locations as possible, because the third trend was less easily interpreted. For two probe locations, $G28C_{SCN}$ and $Y31C_{SCN}$, while each single Rap mutation caused a large shift in vibrational absorption energy, the double mutant Rap E30D/K31E behaved essentially identically to WT Rap. We have found no structural cause for this behavior. These residues may simply be unimportant for the formation of the Rap−Ral interface, and changes in the electrostatic field measured by probes at these locations may not be correlated with changes in Rap−Ral interface formation.

In summary, this study demonstrates that while VSE spectroscopy is a useful tool for examining molecular-level mechanisms of electrostatic events in complex biological systems, the convolution of distance, orientation, and charge in determining the change in local electrostatic field actually experienced by the nitrile probe needs to be carefully interpreted. Observation of reversion behavior in the double mutant Rap E30D/K31E with the probes Ralβ $N27C_{SCN}$ and $N29C_{SCN}$ strongly supports the role these two positions play in supporting an electrostatic mechanism of functional discrimination in GTPase−effector binding. Although these probe locations displayed the reversion mutation behavior that we were predicting when designing these experiments, the convolution of structure and sensitivity to mutations on the surface of Rap demonstrate that unambiguous measurements of electrostatic effects at the Rap−Ral interface will be difficult to achieve. Molecular dynamics sampling appears to be particularly useful in selection of appropriately placed VSE probes. Further experiments on WT and mutant Rap will be guided by extensive MD and continuum electrostatic calculations and are currently underway in our laboratory.

■ ASSOCIATED CONTENT

Ⓢ Supporting Information

Analysis of the convergence of our molecular dynamics simulations, a detailed discussion of the calculation of azimuthal and polar angles, and a description of our absorption spectra fitting procedure. This material is available free of charge via the Internet at http://pubs.acs.org.

■ AUTHOR INFORMATION

Corresponding Author

*E-mail: lwebb@cm.utexas.edu.

Notes

The authors declare no competing financial interest.

■ ACKNOWLEDGMENTS

This work was supported by the Burroughs Wellcome Fund (Grant 1007207.01) and The Welch Foundation (Grant F-1722). L.J.W. holds a Career Award at the Scientific Interface from the Burroughs Wellcome Fund and is an Alfred P. Sloan Research Fellow. The Institute for Cell and Molecular Biology at The University of Texas at Austin is thanked for providing the fluorimeter for kinetics measurements. The authors acknowledge the Texas Advanced Computing Center (TACC) at The University of Texas at Austin for providing high-performance computing resources that have contributed to the results reported within this paper. Ms. Margaret Jameson is thanked for help in expressing and purifying Rap mutants.

■ REFERENCES

(1) Krauss, G. *Biochemistry of Signal Transduction and Regulation*, 3rd ed.; Wiley-VCH Verlag: Weinheim, Germany, 2003.
(2) Nassar, N.; Horn, G.; Herrmann, C.; Scherer, A.; McCormick, F.; Wittinghofer, A. *Nature* **1995**, *375*, 554−560.
(3) Cox, A. D.; Der, C. J. *Oncogene* **2003**, *22*, 8999−9006.
(4) Downward, J. *Nat. Rev. Cancer* **2002**, *3*, 11−22.
(5) Repasky, G. A.; Chenette, E. J.; Der, C. J. *Trends Cell Biol.* **2004**, *14*, 639−647.
(6) Ahmed, S. M.; Daulat, A. M.; Meunier, A.; Angers, S. *J. Biol. Chem.* **2010**, *285*, 6538−6551.
(7) Bailey, C. L. ; Kelly, P.; Casey, P. J. *Cancer Res.* **2009**, *69*, 4962−4968.
(8) Saavedra, A. P.; Tsygankova, O. M.; Prendergast, G. V.; Dworet, J. H.; Cheng, G.; Meinkoth, J. L. *Oncogene* **2002**, *21*, 778−788.
(9) Huang, L.; Hofer, F.; Martin, G. S.; Kim, S. H. *Nat. Struct. Biol.* **1998**, *5*, 422−426.
(10) Herrmann, C. *Curr. Opin. Struct. Biol.* **2003**, *13*, 122−129.
(11) Rudolph, M. G.; Linnemann, T.; Grunewald, P.; Wittinghofer, A.; Vetter, I. R.; Herrmann, C. *J. Biol. Chem.* **2001**, *276*, 23914−23921.
(12) Stafford, A. J.; Ensign, D. L.; Webb, L. J. *J. Phys. Chem. B* **2010**, *114*, 15331−15344.
(13) Herrmann, C.; Horn, G.; Spaargaren, M.; Wittinghofer, A. *J. Biol. Chem.* **1996**, *271*, 6794−6800.
(14) Ensign, D. L.; Webb, L. J. *Proteins* **2011**, *79*, 3511−3524.
(15) Nassar, N.; Horn, G.; Herrmann, C.; Block, C.; Janknecht, R.; Wittinghofer, A. *Nat. Struct. Biol.* **1996**, *3*, 723−729.
(16) Terada, T.; Ito, Y.; Shirouzu, M.; Tateno, M.; Hashimoto, K.; Kigawa, T.; Ebisuzaki, T.; Takio, K.; Shibata, T.; Yokoyama, S.; et al. *J. Mol. Biol.* **1999**, *286*, 219−232.
(17) Honig, B.; Nicholls, A. *Science* **1995**, *268*, 1144−1149.
(18) Gunner, M. R.; Nicholls, A.; Honig, B. *J. Phys. Chem.* **1996**, *100*, 4277−4291.
(19) Lee, L. P.; Tidor, B. *Protein Sci.* **2001**, *10*, 362−377.
(20) Simonson, T. *Curr. Opin. Struct. Biol.* **2001**, *11*, 243−252.
(21) Villa, J.; Warshel, A. *J. Phys. Chem. B* **2001**, *105*, 7887−7907.
(22) Warshel, A.; Papazyan, A. *Curr. Opin. Struct. Biol.* **1998**, *8*, 211−217.
(23) Andrews, S. S.; Boxer, S. G. *J. Phys. Chem. A* **2000**, *104*, 11853−11863.
(24) Andrews, S. S.; Boxer, S. G. *J. Phys. Chem. A* **2002**, *106*, 469−477.
(25) Fafarman, A. T.; Webb, L. J.; Chuang, J. I.; Boxer, S. G. *J. Am. Chem. Soc.* **2006**, *128*, 13356−13357.
(26) Suydam, I. T.; Boxer, S. G. *Biochemistry* **2003**, *42*, 12050−12055.
(27) Suydam, I. T.; Snow, C. D.; Pande, V. S.; Boxer, S. G. *Science* **2006**, *313*, 200−204.
(28) Webb, L. J.; Boxer, S. G. *Biochemistry* **2008**, *47*, 1588−1598.

(29) Fafarman, A. T.; Boxer, S. G. *J. Phys. Chem. B* **2010**, *114*, 13536−13544.
(30) Fafarman, A. T.; Sigala, P. A.; Herschlag, D.; Boxer, S. G. *J. Am. Chem. Soc.* **2010**, *132*, 12811−12813.
(31) Waegele, M. M.; Culik, R. M.; Gai, F. *J. Phys. Chem. Lett.* **2011**, *2*, 2598−2609.
(32) Case, D. A.; Darden, T. A.; Cheatham, T. E.; Simmerling, C. L.; Wang, J.; Duke, R. E.; Luo, R.; Walker, R. C.; Zhang, W.; Merz, K. M.; et al. *AMBER 11*; University of California: San Francisco, 2010.
(33) Dames, S. A.; Kammerer, R. A.; Wiltscheck, R.; Engel, J.; Alexandrescu, A. T. *Nat. Struct. Biol.* **1998**, *5*, 687−691.
(34) Luo, R.; Mann, B.; Lewis, W. S.; Rowe, A.; Heath, R.; Stewart, M. L.; Hamburger, A. E.; Sivakolundu, S.; Lacy, E. R.; Bjorkman, P. J.; et al. *EMBO J.* **2005**, *24*, 34−43.
(35) Phelan, M. M.; Thai, C. T.; Soares, D. C.; Ogata, R. T.; Barlow, P. N.; Bramham, J. *J. Biol. Chem.* **2009**, *284*, 19637−19649.
(36) McCleverty, C. J.; Columbus, L.; Kreusch, A.; Lesley, S. A. *Protein Sci.* **2008**, *17*, 869−877.
(37) Humphrey, W.; Dalke, A.; Schulten, K. *J. Mol. Graphics* **1996**, *14*, 33−38.
(38) van der Spoel, D.; Lindahl, E.; Hess, B.; Groenhof, G.; Mark, A. E.; Berendsen, H. J. C. *J. Comput. Chem.* **2005**, *26*, 1701−1718.
(39) *The PyMOL Molecular Graphics System*, version 1.3r1; Schrödinger LLC: New York, 2010.
(40) Jorgensen, W. L.; Chandrasekhar, J.; Madura, J. D.; Impey, R. W.; Klein, M. L. *J. Chem. Phys.* **1983**, *79*, 926−935.
(41) Roux, B. *Comput. Phys. Commun.* **1995**, *91*, 275−282.
(42) Gallicchio, E.; Andrec, M.; Felts, A. K.; Levy, R. M. *J. Phys. Chem. B* **2005**, *109*, 6722−6731.
(43) Geyer, M.; Herrmann, C.; Wohlgemuth, S.; Wittinghofer, A.; Kalbitzer, H. R. *Nat. Struct. Biol.* **1997**, *4*, 694−699.